arXiv:1602.03326v1 [nucl-th] 10 Feb 2016

Toroidal resonance: relation to pygmy mode, vortical properties and anomalous deformation splitting

V.O. Nesterenko[1], J. Kvasil[2], A. Repko[2,3], W. Kleinig[1], and P.-G. Reinhard[4]
[1] *Laboratory of Theoretical Physics, Joint Institute for Nuclear Research, Dubna, Moscow region, 141980, Russia**
[2] *Institute of Particle and Nuclear Physics, Charles University, CZ-18000, Prague, Czech Republic*
[3] *Department of Nuclear Physics, Institute of Physics SAS, 84511, Bratislava, Slovakia and*
[4] *Institut für Theoretische Physik II, Universität Erlangen, D-91058, Erlangen, Germany*

We review a recent progress in investigation of the isoscalar toroidal dipole resonance (TDR). A possible relation of the TDR and low-energy dipole strength (also called a pygmy resonance) is analyzed. It is shown that the dipole strength in the pygmy region can by understood as a local manifestation of the collective vortical toroidal motion at the nuclear surface. Application of the TDR as a measure of the nuclear dipole vorticity is discussed. Finally, an anomalous splitting of the TDR in deformed nuclei is scrutinized.

I. INTRODUCTION

Over the last years there is a high interest in the investigation of exotic E1 modes, pygmy dipole resonance (PDR), compression dipole resonance (CDR), and toroidal dipole resonance (TDR), see e.g. reviews [1, 2]. The schematic images of these modes are illustrated in Fig. 1.

PDR is the working title of a collection of marked dipole strength at energies below the dipole giant resonance. Although the sub-peaks in the PDR region can have different microscopic structure, one often visualizes their averaged flow pattern as oscillations of the neutron excess against the nuclear core with N=Z [1]. So this resonance can exist only in nuclei with large neutron excess. As seen from Fig. 1a), the schematic PDR flow is irrotational. This resonance gathers effects from various nuclear matter properties (symmetry energy, incompressibility, effective masses) [3] and so can provide useful complementing information on the nuclear equation of state and thus for astrophysical applications.

The CDR also represents an irrotational flow. It is, as the name says, a dipole mode, but with compressional character becoming apparent in a higher order radial profile [4, 5], see Fig. 1b). This resonance can be used as a source of an additional information on the nuclear incompressibility [1].

Further, the TDR is a remarkable example of *vortical* dipole motion, see Fig. 1c). For the first time, the toroidal fraction of the nuclear convection current was inspected by V.M. Dubovik and A.A. Cheshkov [6]. Later S.F. Semenko predicted the TDR in atomic nuclei [7]. The TDR is related to CDR [1, 8, 9]. In the isoscalar (T=0) channel, both resonances constitute the low-energy (TDR) and high-energy (CDR) parts of the isoscalar giant dipole resonance (ISGDR) observed in (α, α') reaction [10]. After extraction of the center-of-mass corrections (cmc), the TDR and CDR become the dominant dipole modes in the isoscalar channel.

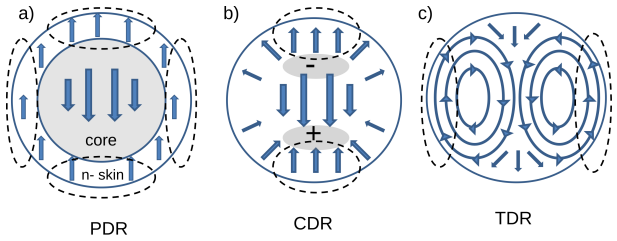


FIG. 1: Schematic velocity fields for the PDR (a), high-energy CDR (b), and TDR (c) flows. The driving field is directed along z-axis. The arrows indicate only directions of the flows but not their strength. In the plot (b), the compression (+) and decompression (-) regions, characterized by increased and decreased density, are marked. The dash curves represent the surface regions where the PDR and CDR/TDR flows are similar.

All three exotic modes, PDR, CDR and TDR, have isoscalar (T=0) and isovector (T=1) branches [1, 2, 9]. In the present review, we will concentrate on the isoscalar branches of the modes. They are easier accessible in scattering experiments and, as shown below, deliver indeed rich physics. Some properties of the PDR/CDR/TDR were already discussed in the literature [1, 2]. In particular, a modest collectivity of the modes were established and it was worked out that complex configurations play a crucial role in formation of the fine structure of the strengths . In the present review, we will focus on the vortical representative of this family - isoscalar TDR [9, 11]. Namely, we will outline some fascinating features of this TDR, recently explored by our group: relation to the PDR [12, 13], possibility to use TDR as a measure of the dipole nuclear vorticity [14], and anomalous deformation splitting of the TDR [15]. The analysis is based on the self-consistent calculations within the Skyrme Quasiparticle Random-Phase-Approximation (QRPA) approach [16–18] with the factorized [19, 20] and exact [21] residual interaction.

The paper is organized as follows. In Section 2, the basic formalism for the TDR and CDR is given. The calculation scheme is outlined. In Section 3, we demonstrate

*Electronic address: nester@theor.jinr.ru

that the PDR can be treated as a manifestation of the TDR at the nuclear surface. In Section 4, the possibility to use the toroidal strength as a measure of the nuclear dipole vorticity is discussed. It is shown that this prescription is more accurate and robust than the familiar Ravenhall-Wambach recipe [22]. In Section 5, we inspect the anomalous deformation splitting of the TDR in axial nuclei (an opposite order of K-branches as compared to the case of the giant dipole resonance - GDR). This feature can be used as an unambiguous fingerprint of the TDR in experiment. Finally, in Section 6 the summary is done.

II. BASIC FORMALISM AND CALCULATION SCHEME

A. Multipole toroidal and compression operators

In the long-wave approximation ($k \to 0$), the standard electric multipole operator reads

$$\hat{M}(E\lambda\mu, k) \approx \hat{M}(E\lambda\mu) + k\,\hat{M}_{\rm tor}(E\lambda\mu) \qquad (1)$$

where

$$\begin{aligned}\hat{M}(E\lambda\mu) &= -\frac{i}{kc}\int d^3r\,(\nabla\cdot\hat{\mathbf{j}}_{\rm nuc})r^\lambda Y_{\lambda\mu} \\ &= -\int d^3r\,\hat{\rho}\,r^\lambda Y_{\lambda\mu} \qquad (2)\end{aligned}$$

is the familiar electric operator and

$$\begin{aligned}\hat{M}_{\rm tor}(E\lambda\mu) &= \frac{i}{2c(\lambda+1)(2\lambda+3)} \qquad (3)\\ &\cdot\int d^3r\hat{\mathbf{j}}_{\rm nuc}\cdot[\,\nabla\times\,(\mathbf{r}\times\nabla)r^{\lambda+2}Y_{\lambda\mu}] \\ &= -\frac{1}{2c}\sqrt{\frac{\lambda}{\lambda+1}}\,\frac{1}{2\lambda+3}\int d^3r\,r^{\lambda+2}\mathbf{Y}_{\lambda\lambda\mu} \\ &\cdot\left(\nabla\times\hat{\mathbf{j}}_{\rm nuc}\right) \qquad (4)\end{aligned}$$

is the toroidal operator [6, 7, 9]. Here $\hat{\mathbf{j}}_{\rm nuc}(\mathbf{r}) = \hat{\mathbf{j}}_{\rm c}(\mathbf{r}) + \hat{\mathbf{j}}_{\rm m}(\mathbf{r})$ is the operator of the nuclear current consisting of convection and magnetization parts. Further, $\hat{\rho}$ is the density operator, $\mathbf{Y}_{\lambda\lambda\mu}(\hat{\mathbf{r}})$ and $Y_{\lambda\mu}(\hat{\mathbf{r}})$ are vector and ordinary spherical harmonics. For the sake of brevity, we will skip below (up to the cases of a possible confusion) the coordinate dependence in currents, densities and spherical harmonics.

Equation (1) shows that the toroidal operator comes as a second order ($\sim k^2$) correction to the dominant electric operator (2). Being determined by the curl of the nuclear current $\left(\nabla\times\hat{\mathbf{j}}_{\rm c}\right)$, the toroidal flow is obviously vortical and thus decoupled from the continuity equation. So the toroidal operator cannot be presented through the nuclear density alone and needs the knowledge of the current distribution.

The multipole compression operator reads [4, 5, 9]

$$\begin{aligned}\hat{M}_{\rm CM}(E\lambda\mu) &= -\frac{i}{2c(2\lambda+3)}\int d^3r r^{\lambda+2}Y_{\lambda\mu} \\ &\cdot\left(\nabla\cdot\hat{\mathbf{j}}_{\rm nuc}\right) \qquad (5)\\ &= -k\frac{1}{2(2\lambda+3)}\int d^3r\hat{\rho}r^{\lambda+2}Y_{\lambda\mu} \qquad (6)\\ &= -k\hat{M}'_{\rm CM}(E\lambda\mu)\,, \qquad (7)\end{aligned}$$

where $\hat{M}'_{\rm CM}(E\lambda\mu)$ is its familiar density-dependent form [4, 5]. The compression operator appears as a probe operator for excitation of the ISGDR [4, 5]. Unlike the toroidal one, this operator may be presented in both current- and density-dependent forms. The operator is determined by the divergence of current $\left(\nabla\cdot\hat{\mathbf{j}}_{\rm c}\right)$ and so is irrotational.

Note that, though the toroidal and compression operators represent essentially different flows, they are closely related. Accordingly there is a coupling between the TDR and CDR [9].

B. E1(T=0) case

Now we will focus on the isoscalar dipole E1(T=0) excitations. Following [9], the role of the magnetization nuclear current for TDR and CDR in E1(T=0) channel is negligible. So only the convection part $\hat{\mathbf{j}}_{\rm c}$ of the nuclear current is considered below.

In E1(T=0) channel, the toroidal and compression operators are reduced to [9, 11, 12, 14, 15]

$$\begin{aligned}\hat{M}_{\rm tor}(E1\mu) &= -\frac{i}{2\sqrt{3}c}\int d^3r\hat{\mathbf{j}}_c \qquad (8)\\ &\cdot[\frac{\sqrt{2}}{5}r^2\mathbf{Y}_{12\mu} + (r^2-\langle r^2\rangle_0)\mathbf{Y}_{10\mu}], \\ \hat{M}_{\rm com}(E1\mu) &= -\frac{i}{2\sqrt{3}c}\int d^3r\hat{\mathbf{j}}_c \qquad (9)\\ &\cdot[\frac{2\sqrt{2}}{5}r^2\mathbf{Y}_{12\mu} - (r^2-\langle r^2\rangle_0)\mathbf{Y}_{10\mu}], \\ \hat{M}'_{\rm com}(E1\mu) &= \frac{1}{10}\int d^3r\hat{\rho}\,[r^3 - \frac{5}{3}\langle r^2\rangle_0 r]Y_{1\mu}\,. \qquad (10)\end{aligned}$$

Here $\langle r^2\rangle_0 = \int d^3r\rho_0 r^2/A$ is the ground-state squared radius, $\rho_0(\mathbf{r})$ is the ground state density, A is the mass number. The operators (8)-(10) have the center of mass correction (c.m.c.) proportional to $\langle r^2\rangle_0$.

The toroidal and compression matrix elements for $E1$ transitions between the ground state $|0\rangle$ and RPA excited state $|\nu\rangle$ are determined through the current transition density (we skip below the index μ)

$$\delta\mathbf{j}_\nu(\mathbf{r}) = \langle\nu|\,\hat{\mathbf{j}}_{\rm c}(\mathbf{r})\,|0\rangle = -i[j^\nu_{10}(r)\,\mathbf{Y}^*_{10} + j^\nu_{12}(r)\,\mathbf{Y}^*_{12}] \quad (11)$$

involving the upper $j_+ = j_{12}$ and lower $j_- = j_{10}$ radial current components. Then

$$\langle\nu|\hat{M}_{\rm tor}(E1)|0\rangle = -\frac{1}{6c}\int drr^2 \cdot [\frac{\sqrt{2}}{5}r^2 j^\nu_{12} + (r^2 - \langle r^2\rangle_0) j^\nu_{10}] , \quad (12)$$

$$\langle\nu|\hat{M}_{\rm com}(E1)|0\rangle = -\frac{1}{6c}\int drr^2 \cdot [\frac{2\sqrt{2}}{5}r^2 j^\nu_{12} - (r^2 - \langle r^2\rangle_0) j^\nu_{10}] . \quad (13)$$

Ravenhall-Wambach proposed that just the current component j_+ determines the vorticity of the dipole motion [22]. Then the flow can be treated as fully vortical ($j_+ \neq 0$, $j_- = 0$), fully irrotational ($j_+ = 0$, $j_- \neq 0$), and mixed ($j_+ \neq 0$, $j_- \neq 0$). Following this prescription, both TDR and CDR are of a mixed (irrotational/vortical) character, which contradicts their predominantly curl- and gradient-like velocities fields exhibited in Fig. 1, see also detailed discussion in [9, 14].

C. Details of the calculation

The calculations were performed within the fully self-consistent Skyrme QRPA method [23]. We use the exact residual interaction for spherical nuclei [21] and the separable residual interaction for axial deformed nuclei [20]. Below these schemes are referred as RPA and SRPA, respectively. Both versions are self-consistent because: i) the mean field and residual interaction are obtained from the same Skyrme functional, ii) the residual interaction includes all the terms of the initial Skyrme functional as well as the Coulomb direct and exchange terms. Both time-even and time-odd densities are take into account. The δ-force volume pairing is treated at the BCS level [24]. The Skyrme force SLy6 [25] providing a satisfactory description of the giant dipole resonance (GDR) [26] is used.

For a deformed nucleus, the equilibrium quadrupole axial deformation β is determined by minimization of the total energy of the system. The SRPA code employs a mesh in cylindrical coordinates.

The calculations use a large configuration space with particle-hole (two-quasiparticle) energies up to 70 MeV. The energy-weighted sum rule for E1(T=1) transitions is fully exhausted. The spurious mode lies around 1 MeV, i.e. safely beyond the TDR and CDR regions.

The toroidal and compression E1(T=0) strength functions read

$$S_\alpha(E1, T=0) = \sum_{\mu,\nu} |\langle\nu|\hat{M}_\alpha(E1\mu)|0\rangle|^2 \zeta(E - E_\nu) \quad (14)$$

where $\hat{M}_\alpha(E1\mu)$ is the toroidal ($\alpha = {\rm tor}$) or compression ($\alpha = {\rm com}$) transition operator given by expressions (8) and (9), respectively. The neutron and proton effective charges are $e^{\rm eff}_n = e^{\rm eff}_p = 1$. The sum in (14) runs through all the QRPA ν-states. Further, $\zeta(E - E_\nu)$ is a Lorenz weight with the averaging parameter Δ. The folding by the Lorentz function simulates the smoothing effects beyond QRPA (coupling to complex configurations and escape widths). In SRPA calculation for axial deformed nuclei, we use the constant averaging parameter Δ=1 MeV [20]. This suffices to demonstrate the deformation splitting of the TDR, discussed in Sec. 5. However our RPA code for spherical nuclei allows to use a more reasonable Lorentz double folding exhibiting a linear dependence of Δ on the excitation energy E above the first emission threshold [21, 27]. This folding is implemented in strength distributions discussed in Sec. 3.

For the description of the GDR and PDR, we calculate within the RPA the photoabsorption $\sigma_\gamma(E1, T=1)$ [28]. The neutron and proton effective charges $e^{\rm eff}_n = -Z/A$ and $e^{\rm eff}_p = N/A$ are used. The Lorentz energy dependent double folding [21] is applied.

More details on the calculation scheme can be found elsewhere [9, 11, 12, 14, 15].

III. RELATION OF THE TOROIDAL AND PYGMY MODES

In the studies [12, 13], it was reported that the PDR and TDR occupy the same energy region and thus are related. This point was thoroughly investigated for a doubly magic nucleus ^{208}Pb. The strength functions, transition densities and current fields were inspected. The calculations confirmed the experimental finding [29] that the PDR is separated into isoscalar lower-energy and mixed (isoscalar/isovector) higher-energy branches. The main attention was paid to the low-energy isoscalar part of the PDR [12, 13]. It was shown that though the transition densities in this energy region are typical for the PDR (dominance of the neutron flow at the nuclear surface), the corresponding current fields (current transition densities) are obviously of toroidal character. Thus it was suggested that the PDR is a peripheral manifestation of the toroidal flow.

At first glance, this suggestion looks incorrect because PDR and TDR represent essentially different irrotational and vortical kinds of nuclear motion. This is clearly seen in the panels a) and c) of Fig. 1. However the same panels indicate that both motions are quite similar at the nuclear surface, see left and right boundary regions marked by the dash curves. So the PDR could be a local peripheral manifestation of the TDR. Following Fig. 1, PDR and CDR flows are similar at the top and bottom boundary regions. So perhaps the PDR has also some dipole compression fraction.

In this section, we briefly repeat the above analysis but now for a doubly-magic nucleus ^{132}Sn characterized by a significant neutron excess. Let's first consider the relevant strength functions exhibited in Fig. 2. In the panel a) the photoabsorption σ_γ embracing the GDR and

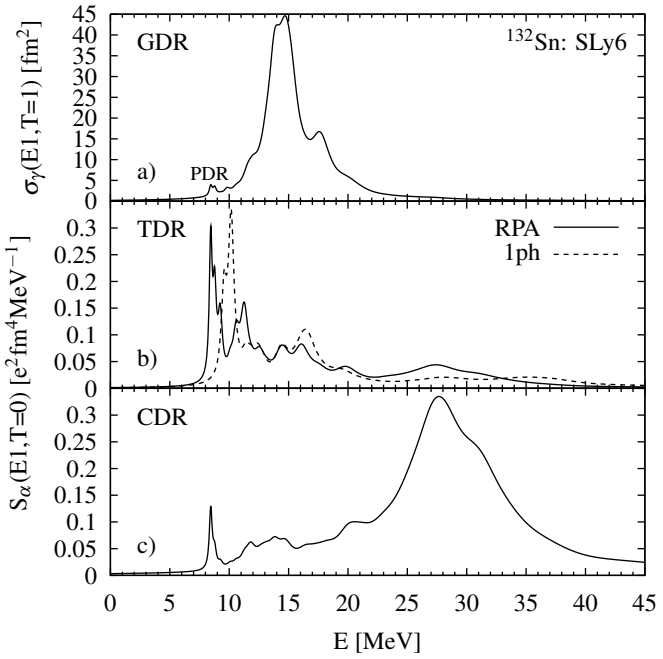


FIG. 2: The dipole strengths calculated within RPA with the force SLy6 in in ^{132}Sn: the photoabsorption embracing the GDR and PDR (a); the E1(T=0) strength functions (14) for the TDR (b)and CDR (c). The panel (b) also shows the 1ph strength depicted by the dash line.

PDR is shown. The toroidal and compression strengths (14) are given in the panels b)-c). It is easy to see that PDR and low-energy TDR/CDR peaked parts share the same energy region and so can be coupled. The panel b) also shows the particle-hole (1ph) unperturbed toroidal strength. One sees that, in the RPA case, the low-energy TDR peak is significantly downshifted relative to its 1ph counterpart. This signals a noticeable collectivity of the TDR.

More detailed information of the dipole strength in this energy region can be obtained from the inspection of the transition densities (TD) and current fields (CF). Note that TD and CF do not depend on the toroidal (8) and compression (9) operators and are fully determined by the RPA wave functions. It is not worth to consider these patterns for individual ν-states because they can vary from state to state and so hide common features of the flow. Instead we consider TD and CF properly averaged (summed) over a relevant energy intervals. The technique of computing of the summed TD/CF is described in detail in [12]. Note that this technique circumvents a possible ambiguity in the signs of the RPA wave functions. In the present study for ^{132}Sn, the TD/CF are calculated at the energy interval 6-10 MeV covering the PDR and low-energy TDR and CDR peaks.

Figure 3 shows the RPA and 1ph proton and neutron transition densities in ^{132}Sn. In the RPA case, we see a typical picture when the proton and neutron TD are strong and in phase inside the nucleus (r ∼4-6 fm) but

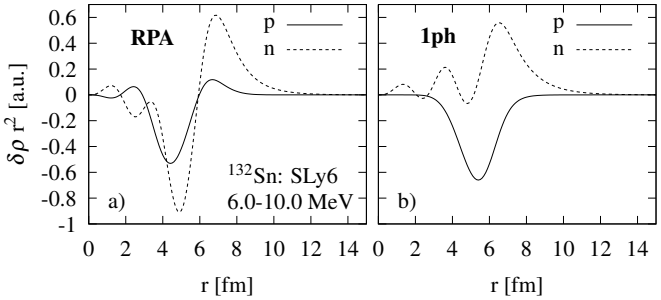


FIG. 3: RPA (left) and 1ph (right) r^2-weighted proton (solid curve) and neutron (dash curve) transition densities in ^{132}Sn, calculated with the force SLy6. The TD are summed in the energy interval 6-10 MeV.

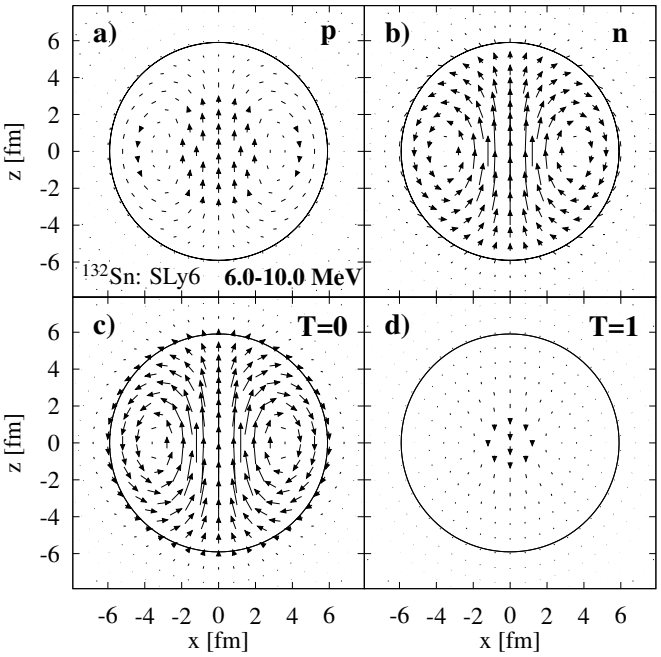


FIG. 4: The proton (a), neutron (b), isoscalar (c) and isovector (d) current fields calculated within RPA in ^{132}Sn. The CF are summed in the energy interval 6-10 MeV.

the neutron TD strictly dominates at the nuclear boundary (r ∼6-10 fm). Just this TD behavior is often used as a justification of the PDR view in terms of the oscillation of the neutron excess against the N=Z core, see Fig. 1a). A noticeable difference between the RPA and 1ph TD indicates that the impact of the residual interaction is important.

The TD are still too rough characteristics since they illustrate only a radial dependence of the flow but not its angular distribution. At the same time, the latter is crucial to recognize the actual flow pattern. Thus we have to inspect the CF which reveal more details. The CF for the energy interval 6-10 MeV in ^{132}Sn are exhibited in Fig. 4. The proton, neutron, isoscalar, and isovector flows at the plane $z - x$ are shown. We see that the nuclear motion at 6-10 MeV has a clear isoscalar toroidal

character, cf. with Fig. 1c). So it is quite possible that the PDR is rooted in the TDR and is actually its manifestation at the nuclear surface (where both PDR and TDR flows look as similar irrotational patterns) if the surface is dominated by neutron density. Note that by definition the PDR exists only in nuclei with a neutron excess. Instead the TDR is a general feature of all the nuclei including those with N=Z.

The total PDR, with its isoscalar and mixed parts, is probably a complicated mixture of different kinds of the dipole motion: toroidal, compression, GDR tail, etc [12, 13]. However our analysis of CF obviously shows that the toroidal contribution is of a prior importance. All the dipole motions should be coupled and so generated simultaneously in various reactions. A ratio between their contributions in the dipole response should depend on the applied reaction (photoabsorption, (α,α'), (e,e'), etc).

Note that some signs of the toroidal flow in the PDR region can be noticed in the velocity fields of previous RPA calculations [8, 30]. A distinctive toroidal motion in the PDR region was obtained in the calculations [31] within the Quasiparticle Phonon Model (QPM) [32]. Besides, the PDR/TDR interplay was recently discussed in the semiclassical exploration [33]. However the studies [8, 30, 31] did not consider a possible relation between PDR and TDR while the study [33] was done at a phenomenological level. Besides, unlike our scheme, the previous RPA and QPM calculations inspected TD/CF for individual states or used summed TD/CF without a special care for an ambiguity in the sign of the dipole states.

IV. TDR AS A MEASURE OF NUCLEAR DIPOLE VORTICITY

There are two basic kinds of the nuclear flow: irrotational and vortical [23, 28]. The irrotational motion is pertinent to collective low-energy excitations and regular electric GR [34]. The vortical flow takes place (besides a plane nuclear rotation) in single-particle excitations [22] and exotic GR like e.g. electric TDR [9, 14] and twist magnetic quadrupole resonance [35]).

Despite some previous studies (see e.g. [22, 36]), our knowledge about nuclear vorticity is still rather poor. Even the measure of the vorticity is disputable. In hydrodynamics, the vorticity is defined as curl of the velocity field [37],

$$\varpi(\mathbf{r}) = \nabla \times \mathbf{v}(\mathbf{r}) \ . \tag{15}$$

However nuclear physics deals not with velocities but currents. In this connection, Ravenhall and Wambach have proposed the j_+-component of the nuclear current as a measure and indicator of the nuclear vortcity (to be called below as RW vorticity) [22]. They have shown that j_+ is unrestricted by the continuity equation (CE)

$$\delta\dot{\rho}_\nu(\mathbf{r}) + \nabla \cdot \delta\mathbf{j}_\nu(\mathbf{r}) = 0 \tag{16}$$

in the integral sense and so is suitable for a divergence-free (vortical) pattern [22].

For a long time, the RW prescription was used for estimation of the vortical contribution in various excitations, see e.g. [31]. However our last studies have shown that this prescription has serious shortcomings [9, 14]. In particular, the RW scheme obviously fails for the TDR and CDR. Indeed, following Eqs. (12)-(13), these modes involve both j_+ and j_- components of the nuclear current and so have to be of a mixed (irrotational/vortical) nature. At the same time, the TDR is basically vortical while the CDR is irrotational. Their velocities are the gradient and curl functions, respectively [9]. And their current fields closely correspond to vortical and irrotational images given in Fig. 1.

Moreover, the thorough analysis of the current components $j_-(\mathbf{r}) = j^\nu_{10}(r)\ \mathbf{Y}^*_{10}$ and $j_+(\mathbf{r}) = j^\nu_{12}(r)\ \mathbf{Y}^*_{12}$ has shown that both them have strong contributions in the low-energy toroidal and high-energy compression regions [14]. Besides, the divergences and curls of these components turned out to be of the same order of magnitude. This means that j_+ has no any strong advantage over j_- to represent the nuclear vorticity. Neither j_+ nor j_- alone can represent a vortical or irrotational flow. Instead Eqs. (12) and (13) suggest that only the proper combinations of j_+ are j_- are suitable for these aims.

In this connection, we propose the toroidal strength as a natural and robust measure of the nuclear vorticity. Following Eqs. (12), the toroidal matrix element is determined by the combination of δj_+ and δj_-, resulting in a clear vortical flow demonstrated in Figs. 4. Besides, as shown in [14], the toroidal and hydrodynamical criteria of the vorticity are closely related.

One may also provide some formal arguments to justify the toroidal pattern as the standard for vorticity. We know that the electric current transition density is decomposed into longitudinal and transversal components,

$$\delta\mathbf{j}(\mathbf{r}) \ = \ \delta\mathbf{j}_\parallel(\mathbf{r}) + \delta\mathbf{j}_\perp(\mathbf{r}) \ , \tag{17}$$

$$\delta\mathbf{j}_\parallel(\mathbf{r}) \ = \ \nabla\phi(\mathbf{r}), \quad \delta\mathbf{j}_\perp(\mathbf{r}) = \nabla \times \nabla \times (\mathbf{r}\chi(\mathbf{r})), \tag{18}$$

where $\phi(\mathbf{r})$ and $\chi(\mathbf{r})$ are some scalar functions [6]. As compared to the prescription [22], this definition looks more plausible for the search of CE-unrestricted divergence-free current because we immediately obtain $\delta\mathbf{j}_\perp$ as a natural candidate.

The current components can be expanded in the basis of eigenfunctions $\mathbf{J}^{(\kappa)}_{\lambda\mu k}(\mathbf{r})$ (κ = -, 0, +) of the vector Helmholtz equation (in analogy to the expansion of the vector-potential, in [38]). Then the transversal component reads

$$\delta\mathbf{j}_\perp(\mathbf{r}) = \sum_{\lambda\mu k} \mathbf{J}^{(+)}_{\lambda\mu k}(\mathbf{r})\ m^{(+)}_{\lambda\mu}(k) \tag{19}$$

where $m^{(+)}_{\lambda\mu}(k)$ is the electric transversal form-factor and integration by k is assumed. In the long-wave approximation ($k \to 0$), the transversal component is reduced

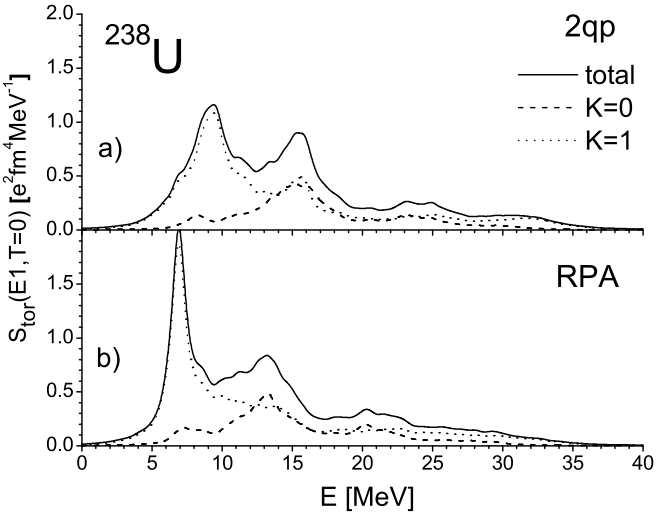


FIG. 5: 2qp (a) and SRPA (b) TDR strength functions calculated with the force SLy6 in ^{238}U. In both panels, the total strength (solid curve) and its K=0 (dash curve) and K=1 (dotted curve) branches are depicted.

to the longitudinal one. After subtraction of this long-wave part from $\delta\mathbf{j}_\perp$, we get at $k > 0$ the toroidal current density [6]. The transversal character of such toroidal current is confirmed by expression (3). Being independent from $\delta\mathbf{j}_\parallel$ and thus decoupled from CE, the toroidal current is a relevant vortical part of the complete nuclear current, suitable as a robust measure of the nuclear vorticity.

V. ANOMALOUS DEFORMATION SPLITTING OF TDR

The GDR in axial nuclei exhibits the deformation splitting into K=0 and K=1 branches [39]. In prolate nuclei, the branch K=0 has a lower energy than the K=1 one, $E_{K=0} < E_{K=1}$. The opposite sequence, $E_{K=1} < E_{K=0}$, takes place in oblate nuclei. This splitting can be easily explained in terms of dipole oscillations along z- and x, y-axes.

The deformation splitting should also take place in the TDR. However, the calculations for the TDR (prolate ^{170}Yb [15]) have surprisingly revealed an anomalous sequence $E_{K=1} < E_{K=0}$, i.e. opposite to the order typical for GDR in oblate axial nuclei. It was shown that this sequence takes place in both SRPA and 2qp toroidal strength functions. So the effect is not caused by the residual interaction.

Here we discuss the anomalous deformation splitting of TDR in prolate ^{238}U. The corresponding SRPA and two-quasiparticle (2qp) strength functions are depicted in Fig. 5. The strengths are smoothed by a Lorentz weight with the constant averaging parameter Δ= 1 MeV. The deformation parameter β=0.286 is obtained by minimization of the total energy of the system. Note that the calculated β excellently reproduces the experimental value $\beta_{\rm exp}$=0.2863(24) [40].

Figure 5 shows that, in accordance with previous results for rare-earth nuclei [15], the TDR in ^{238}U also exhibits the anomalous splitting. Indeed, in RPA case, the main K=1 peak lies significantly lower (5-10 MeV) than the main K=0 peak (10-17 MeV). In the low-energy region 5-12 MeV, the K=1 strength strongly dominates over K=0 one. Though both branches are distributed in a wide energy interval and have more or less the same strength at E> 12 MeV, it is easy to see that the K=1 centroid is certainly lower than the K=0 one. As seen from Fig. 5a), a similar picture emerges for the unperturbed (without residual interaction) two-quasiparticle (2qp) strength.

The anomalous splitting of the TDR might be related with the fact that TDR, unlike the regular $E\lambda$ giant resonances determined by $r^\lambda Y_{\lambda\mu}$-fields, is not the Tassie mode. Following (3), the toroidal multipole field rather includes $r^{\lambda+2}Y_{\lambda\mu}$. This means that simple arguments explaining the deformation splitting in the GDR do not work here. However, following expression (6), the CDR is also not the Tassie mode. At the same time, the calculations do not show in the CDR the distinctive "opposite order" splitting in deformed nuclei [42]. Perhaps here the vortical character of the TDR is a decisive factor. This problem deserves further exploration. Anyway, the anomalous splitting of the TDR can be used for its experimental discrimination from other dipole modes.

VI. SUMMARY

Some remarkable properties of the isoscalar toroidal dipole resonance (TDR), recently studied by our group, were briefly discussed. The main attention was paid to a) the relation of the TDR and low-energy dipole strength (also denoted as PDR) [12], b) the possibility to use the toroidal flow as a measure of the nuclear dipole vorticity [14], and c) anomalous deformation splitting of the TDR [15]. The analysis was based on the calculations within the self-consistent quasiparticle random-phase-approximation (QRPA) method [23] with the Skyrme force SLy6 [25]. Two QRPA versions, exact RPA for spherical nuclei [21] and separable RPA (SRPA) for deformed nuclei [20] were used. As relevant examples, the spherical ^{132}Sn and deformed ^{238}U were considered. The vortical TDR was discussed together with its irrotational counterpart, the compression dipole resonance (CDR).

Our study has confirmed previous findings [9, 12, 14, 15]. Namely, for the case of ^{132}Sn, we showed that the TDR and PDR share the same energy region. The field of the nuclear convection current in this region is clearly toroidal. Both TDR and PDR flows have much in common at the nuclear surface. So it is quite possible that the PDR is actually a local manifestation of the TDR at the nuclear boundary.

Besides we presented the arguments that the familiar measure of the nuclear vorticity proposed by Ravenhall and Wambach [22] (j_+ component of the nuclear current) is not relevant and obviously fails in the TDR/CDR case. Instead, the toroidal current and strength are much better suited for this aim.

Finally, using the SRPA results for ^{238}U, we considered the anomalous deformation splitting of the TDR. In accordance to previous study [15], we have found that in prolate ^{238}U the K=1 branch of the TDR has lower energy than the K=0 branch, i.e. we received the opposite order of the branches as compared to the regular giant dipole resonance. The nature of this feature is not yet clear and needs a further study. Anyway this feature may be used for an experimental discrimination of the TDR.

Note that for dipole excitations in the PDR region the coupling with complex configurations (CCC) can be important [29, 43, 44]. However, we think that the toroidal features we have found are too strong to be spoiled by this effect. This is confirmed e.g. by QPM calculations which include the CCC [31] but nevertheless report a strong toroidal flow at the PDR region.

The isoscalar TDR and CDR dominate the E1(T=0) channel and can be observed in (α, α') reaction, see e.g. [10]. So, despite of their second-order character [9], the PDR and CDR are accessible and important examples of the dipole excitations. The TDR is the only vortical mode in E1(T=0) channel. The TDR and PDR share the same energy region and are certainly related. Now the PDR is intensively investigated as it provides an important information for the nuclear equation of state and astrophysical applications [1, 2]. The analysis of the TDR/PDR interplay can be essential for a better understanding of the PDR features and related topics.

Acknowledgments

The work was partly supported by DFG (RE 322/14-1), Heisenberg-Landau (Germany-BLTP JINR), and Votruba - Blokhintsev (Czech Republic - BLTP JINR) grants. J.K. and A.R. are grateful for the support of the Czech Science Foundation (P203-13-07117S).

[1] N. Paar, D. Vretenar, E. Khan, and G. Colo, Rep. Prog. Phys. **70**, 691 (2007).
[2] D. Savran, T. Aumann, and A. Zilges, Prog. Part. Nucl. Phys. **70**, 210 (2013).
[3] P.-G. Reinhard and W. Nazarewicz, Phys. Rev. C**87**, 014324 (2013).
[4] M.N. Harakeh et al, Phys. Rev. Lett. **38**, 676 (1977).
[5] S. Stringari, Phys. Lett. B**108**, 232 (1982).
[6] V.M. Dubovik and A.A. Cheshkov, Sov. J. Part. Nucl. **5**, 318 (1975).
[7] S.F. Semenko, Sov. J. Nucl. Phys. **34**, 356 (1981).
[8] D. Vretenar, N. Paar, P. Ring, and G.A. Lalazissis, Phys. Rev. C**63**, 047301 (2001).
[9] J. Kvasil, V.O. Nesterenko, W. Kleinig, P.-G. Reinhard, and P. Vesely, Phys. Rev. C**84**, 034303 (2011).
[10] M. Uchida et al, Phys. Rev. C**69**, 051301(R) (2004).
[11] J. Kvasil, V.O. Nesterenko, A. Repko, W. Kleinig, P.-G. Reinhard, and N. Lo Iudice, Phys. Scr. T**154**, 014019 (2013).
[12] A. Repko, P.-G. Reinhard, V.O. Nesterenko, and J. Kvasil, Phys. Rev. C**87**, 024305 (2013).
[13] V.O. Nesterenko, A. Repko, P.-G. Reinhard, and J. Kvasil, EPJ Web of Conferences **93**, 01020 (2015).
[14] P.-G. Reinhard, V.O. Nesterenko, A. Repko, and J. Kvasil, Phys. Rev. C**89**, 024321 (2014).
[15] J. Kvasil, V.O. Nesterenko, W. Kleinig, and P.-G. Reinhard, Phys. Scr. **89**, 054023 (2014).
[16] T.H.R. Skyrme, Phil. Mag. **1**, 1043 (1956).
[17] D. Vauterin and D.M. Brink, Phys. Rev. C**5**, 626 (1972).
[18] M. Bender, P.-H. Heenen, and P.-G. Reinhard, Rev. Mod. Phys. **75**, 121 (2003).
[19] V.O. Nesterenko, J. Kvasil, and P.-G. Reinhard, Phys. Rev. C**66**, 044307 (2002).
[20] V.O. Nesterenko, W. Kleinig, J. Kvasil, P. Vesely, P.-G. Reinhard, and D.S. Dolci, Phys. Rev. C**74**, 064306 (2006).
[21] A. Repko, J. Kvasil, V.O. Nesterenko, and P.-G. Reinhard, arXiv:1510.01248[nucl-th].
[22] D.G. Ravenhall and J. Wambach, Nucl. Phys. A**475**, 468 (1987).
[23] P. Ring and P. Schuck, *Nuclear Many Body Problem*, (Springer-Verlag, New York, 1980).
[24] M. Bender, K. Rutz, P.-G. Reinhard, and J.A. Maruhn, Eur. Phys. J. A**8**, 59 (2000).
[25] E. Chabanat, P. Bonche, P. Haensel, J. Meyer, and R. Schaeffer, Nucl. Phys. A**635**, 231 (1998).
[26] W. Kleinig, V.O. Nesterenko, J. Kvasil, P.-G. Reinhard, and P. Vesely, Phys. Rev. C**78**, 044313 (2008).
[27] J. Kvasil, V.O. Nesterenko, W. Kleinig, D. Božík, and P.-G. Reinhard, Int. J. Mod. Phys. E. **20**, 281 (2011).
[28] A. Bohr and B.R. Mottelson, *Nuclear Structure* Vol. 2 (Benjamin, New York, 1974).
[29] J. Endres et al, Phys. Rev. Lett. **105**, 212503 (2010).
[30] V.Derya et al, Phys. Lett. B**730**, 288 (2014).
[31] N. Ryezayeva et al, Phys. Rev. Lett. **89**, 272502 (2002).
[32] V.G. Soloviev, *Theory of Atomic Nuclei*, (Oxford, Pergamon Press, 1976).
[33] M. Urban, Phys. Rev. C**85**, 034322 (2012).
[34] M.N. Harakeh and A. van der Woude, *Giant Resonances* (Clarendon Press, Oxford, 2001).
[35] G. Holzwarth and G. Ekart, Z. Phys. A**283**, 219 (1977).
[36] E.C. Caparelli and E.J.V. de Passos, J. Phys. G: Nucl. Part. Phys. **25**, 537 (1999).
[37] L.D. Landau and E.M. Lifshitz, *Course of Theoretical Physics: Hydrodynamics* Vol. 6, (Butterworth-Heinemann, Oxford, 1987).
[38] J.M. Eisenberg and W. Greiner, *Excitation Mechanisms of the Nucleus: Electromagnetic and weak interaction*, (North-Holland, 1988).
[39] M. Danos, Nucl. Phys. **5**, 23 (1958).

[40] S. Raman, C.W. Nestor, Jr., and P. Tikkanen, At. Data Nucl. Data Tables **78**, 1 (2001).
[41] L.J. Tassie, Austr. J. Phys. **9**, 407 (1956).
[42] J. Kvasil, V.O. Nesterenko, W. Kleinig, D. Bozik, P.-G. Reinhard, and N. Lo Iudice, Eur. Phys. J. A**49**, 119 (2013).
[43] E. Litvinova, P. Ring, and V. Tselyaev, Phys. Rev. C**78**, 014312 (2008).
[44] N.N. Arsenyev, A.P. Severyukhin, V.V. Voronov, and Nguen Van Giai, EPJ Web of Conferences **38**, 17002 (2012).